ISSN 1392 - 1207. MECHANIKA. 2011. 17(6): 649-655

Control algorithm to reject the effect of iron sleepers for magnetic levitation vehicle using LSM with PM Halbach and ironless coil

Xiao Zhang, Hu Cheng, Yungang Li

College of Mechatronic Engineering and Automation, National University of Defense Technology, Changsha 410073, China, E-mail: zhangxiao01@163.com

crossref http://dx.doi.org/10.5755/j01.mech.17.6.1009

1. Introduction

In magnetic levitation (maglev) system, suspension, guidance and propulsion are provided by magnetic forces. Basically, there are two kinds of linear motors utilized to provide propulsion force for maglev vehicles [1, 2]. One design is called linear synchronous motor (LSM), and the other is linear induction motor (LIM). LSM possesses the dominant advantage of high efficiency, and is widely applied in high-speed maglev vehicles, such as Germany TR maglev vehicle and Japan MLU/MLX superconductive maglev vehicle. LIM is widely used in low-speed maglev systems, such as Japan HSST maglev vehicle. The reason is that LIM suffers from the influence of eddy current [3], which in return generates acceleration resistance for the maglev vehicle. As the increase of people's demands for rapidity and energy-saving, it is appreciable that the tendency of propulsion system for maglev vehicles is toward LSM.

Typically, LSM in the maglev system is composed of iron coils on the guideway supplying primary magnetic field and electromagnets on the vehicle offering secondary magnetic field. There are energy-consuming in both the electromagnets and the iron coils in this kind of LSM. One method to reduce the energy-consuming on the vehicle is to replace electromagnets with Permanent Magnets (PMs) [4, 5], which can provide field without power supply. The improvement of the performance of PM materials [6] and the present of Halbach array [7] greatly promote the application of PM in LSM. Currently the maximum magnetic energy product of permanent magnets applicable to commercial manufacture has achieved at 397.9 kJ/m^3. And Halbach array is an innovative combination of PMs arranged with different magnetization directions and it can enhance the magnetic field on one side while weaken the magnetic field on the other side. Iron coils should not be utilized if the magnetic field on the vehicle is provided by PM Halbach, or there will be strong attractive force (normal force) between the PMs on the vehicle and the iron on the guideway. Thus LSM with PM Halbach and ironless coil is a good candidate to maglev propulsion system, and it has the characteristics of zero power supply on the vehicle and zero normal force. This innovative structure of LSM has been successfully utilized in American GA maglev vehicle.

The magnetic field and force generated by LSM with PM Halbach and ironless coil are studied in previous literatures. H. Bergh et al. presented the approximate analytical solution to magnetic field of Halbach near the surface and deduced the propulsion and normal force generated by the LSM [8]. To investigate the magnetic field far away from the surface, J.F. Hoburg analyzed the static magnetic field of dual Halbach array for GA maglev vehicle by magnetization charge theory, but the results are quite complicated [9]. C.S. Li et al. investigated the optimization technique of PM Halbach array for electrodynamic suspension (EDS) maglev [10]. Magnetic field and optimization design of rotary motor using PM Halbach are conducted by Z.P. Xia et al. [11] and M. Markovic et al [12]. X. Zhang et al. investigated the magnetic field and the magnetic force of LSM with PM Halbach and ironless coil by introducing surface current theory [13].

However, no attention has been paid to the iron sleepers on the guideway, with which attractive force can be generated between the PM Halbach and the guideway. The direction of this attractive force is opposite to the suspension force, which will increase the suspension load and affect the suspension performance.

This paper focuses on analysis of the effect of the iron sleepers on the suspension system using LSM with PM Halbach and ironless coil and the design of the control strategy to reject this effect. The analytical model of the attractive force is proposed by introducing the approximate analytical expression for the field of PM Halbach. And then the suspension performance under consideration of the iron sleepers on the guideway is testified by simulation, which demonstrates that the effect of iron sleepers on the suspension system cannot be ignored. The control strategy to reject this effect is designed, and its effectiveness is illustrated by simulation.

This paper is organized as follows. Section 2 presents the structure of LSM with PM Halbach and ironless coil, and the iron sleepers on the guideway. Section 3 introduces the analytical description of the magnetic field of PM Halbach, and develops analytical solution to attractive force generated by PM Halbach and iron sleepers. Section 4 investigates the effect of iron sleepers on the suspension system by adding the proposed force to suspension system, and simulation result shows that the attractive force brings resonance to suspension system with typical state feedback controller. In section 5, a nonlinear controller is designed using a feedback linearization technique, and simulation result shows that it is quite effective to reject the resonance resulting from sleepers. Finally, a brief summary are discussed in Section 6.

2. System description

2.1. Structure of the LSM with PM Halbach and the ironless coil

The basic structure of LSM with PM Halbach and ironless coil is shown in Fig. 1 [14]. The PM Halbach is

located under the maglev vehicle, and the ironless coil is installed on the guideway. The magnetization directions of the magnetic cubes in the array among a period are different from each other, and Fig. 1 shows an example that

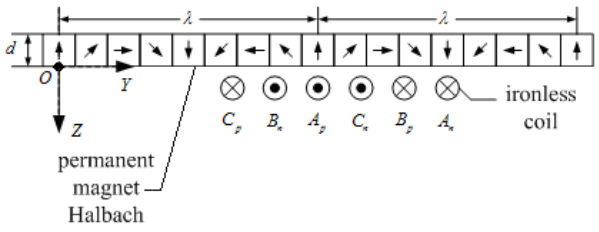

Fig. 1 The structure of LSM with PM Halbach and ironless coil

the magnetization directions change by $\pi/4$ orderly. When three-phase current is added into the ironless coil on the guideway, there will be magnetic forces generated between the vehicle and the guideway. The vertical force acts as normal force, and the horizontal force acts as propulsion force. Under synchronous control strategy, the propulsion force can reach its maximum value while the normal force is zero. Thus the LSM has the characteristics of zero power supply on the vehicle because of PM Halbach array and zero normal force because of ironless coil on the guideway.

2.2. Structure of the iron sleepers on the guideway

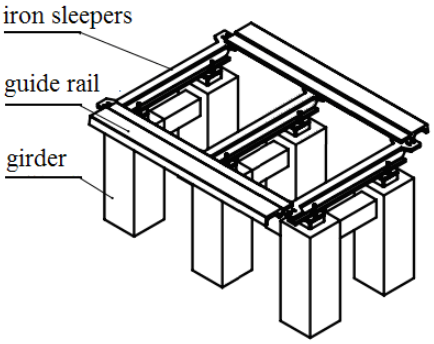

Fig. 2 The simple structure of the iron sleepers on the guideway

The simple structure of the iron sleepers on the guideway is shown in Fig. 2 [15, 16]. The iron sleepers are utilized to connect the guide rail and the girder, and they are periodically distributed along the guideway. As the sleepers are made of iron, attractive force will be generated between the PM Halbach on the vehicle and the iron when the vehicle passes through the guideway. Obviously, the attractive force acting on the vehicle points downwards and it accordingly adds extra suspension load on the vehicle. Moreover, the attractive force acts periodically pulsate, which will continuously affect the performance of the suspension system.

3. Calculation of the force between PM Halbach and the ironless sleepers

The attractive force between the PM Halbach and the iron sleepers acts as magnetic force between PM and ferromagnetic material. The calculation starts from the magnetic field generated by PM Halbach.

3.1. Expression of the magnetic field of the pm halbach

Motors in the maglev vehicle are all linear. The PM Halbach utilized to the LSM is linear Halbach, as shown in Fig. 1. In Fig. 1, the magnetic field under the array is enhanced, while the magnetic field above the array is greatly weakened. Here only the magnetic field on the enhanced side is concerned.

As shown in [8], the peak magnetic field at the surface of Halbach array B_0 can be calculated as

$$B_0 = B_r\left(1-e^{-kd}\right)\frac{sin(\pi/m)}{\pi/m} \tag{1}$$

where B_r is the residual PM flux density, d is the thickness of the array, n is the number of magnets in one period of array, and

$$k = \frac{2\pi}{\lambda} \tag{2}$$

with λ being the wavelength of the Halbach array. The structural parameters λ and d are shown in Fig. 1. From Eq. (1) it can be seen that B_0 is a constant if the structure of the array is established.

Build coordinate Y-O-Z for the array as shown in Fig. 1. The axis OY points rightwards, the axis OZ points downwards, and the origin O locates on the surface of one cube with the magnetization direction pointing upwards. It is known that, the peak of the magnetic field of the array decreases exponentially as the distance from the surface increases. And then the peak magnetic field when the vertical coordinate equals to z is [9]

$$B_m = B_0 e^{-kz} \tag{3}$$

Also it is known that the magnetic field changes sinusoidally along the axis OY and cosinusoidally along the axis OZ. And then the expression of the components of the magnetic field at point (y,z) can be described as [9]

$$\left.\begin{aligned} B_y &= B_m\, sin(ky) \\ B_z &= B_m\, cos(ky) \end{aligned}\right\} \tag{4}$$

3.2. Calculation of the attractive force

The attractive force F between the PM Halbach and the iron sleepers can be approximately established by the following equation [17, 18]

$$F = \frac{B^2 S}{2\mu_0} \tag{5}$$

where B is the magnetic induction, μ_0 is permeability in the vacuum, and S is the area of the ferromagnetic material vertically to the direction of the magnetic field.

The result presented in Eq. (5) is only applicable

to the cases that the magnetic field is evenly distributed. For Eq. (4), the magnetic field changes to the position y. Then the attractive force between the PM Halbach and the iron sleepers should be calculated by implementing integral of y.

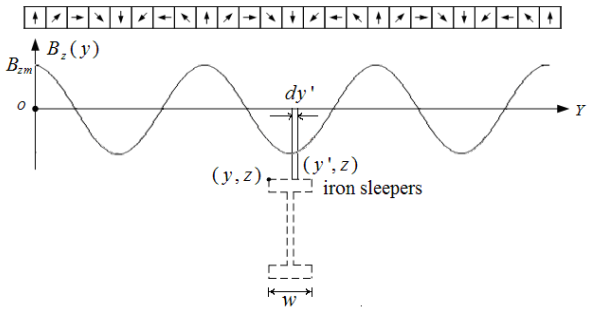

Fig. 3 Diagram used to calculate the attractive force

As shown in Fig. 3, only the magnetic field along z axis B_z contributes to the attractive force. Suppose the length of the Halbach is infinite along Y axis. Consider one piece of iron sleeper, and denote the left of the sleeper locates at (y,z). Choosing an arbitrary point on the surface of the sleeper as (y',z), then from Eq. (5) the forces acts on the area with width dy' is

$$dF_z = \frac{B_z^2 S_{dy'}}{2\mu_0} \tag{6}$$

Supposing the width (the length vertical to the surface of the paper) of the LSM is l, the width of the sleeper is w, and substituting Eqs. (1)-(4) yields

$$dF_z = \frac{B_0^2 l}{2\mu_0} e^{-2kz} cos^2\left(ky'\right) dy' \tag{7}$$

Conducting integral of Eq. (7) with respect to y' yields

$$F_z = \frac{B_0^2 l}{4k\mu_0}\left[sin\left(kw\right)cos\left(2ky+kw\right)+kw\right]e^{-2kz} \tag{8}$$

It can be seen that F_z relates to y and z.

4. Effect of sleepers on the suspension system

4.1. Model of a single-point suspension system

A single-point system is the basic unit for the maglev suspension system, and its structure is shown in Fig. 4, where δ is the suspension gap between the guideway and the magnet, u is the voltage added to the coil, i is the current in the coil, F is the suspension force generated by the electromagnet, m is the mass of the electromagnet, and F_z is the attractive force generated by Halbach array and the iron sleepers.

Choosing the state as $x=\left[\delta \quad \dot{\delta} \quad i\right]^T$, the model of the suspension system can be described as [19, 20]

$$\left.\begin{aligned} \dot{x}_1 &= x_2 \\ \dot{x}_2 &= g - \frac{k_a}{m}\left(\frac{x_3}{x_1}\right)^2 - \frac{F_z}{m} \\ \dot{x}_3 &= \frac{x_2 x_3}{x_1} - \frac{x_1}{2k_a}\left(u - Rx_3\right) \\ y &= x_1 \end{aligned}\right\} \tag{9}$$

where g is the gravity acceleration, R is the resistance of the coil and k_a is a parameter determined by the experimental setup. To investigate the effect of the sleepers, following a full state feedback controller is designed and the control performance is testified for the suspension system Eq. (9) under both $F_z = 0$ and $F_z \neq 0$.

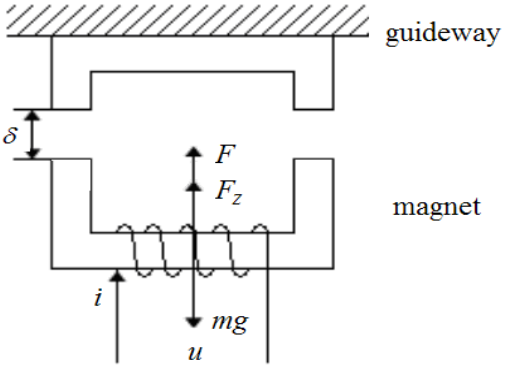

Fig. 4 Structure of a single-point suspension system

4.2. Full state feedback controller design

In experimental setup, the operation point is selected as $\delta_0 = 0.01$ m. Then according to Eq. (9), the equilibrium is [20]

$$\left.\begin{aligned} X_0 &= \left[\delta_0 \quad 0 \quad i_0\right]^T \\ i_0 &= \delta_0\sqrt{\frac{mg}{k_a}} \end{aligned}\right\} \tag{10}$$

Linearizing Eq. (9) at the equilibrium Eq. (10) yields

$$\left\{\begin{aligned} \Delta\dot{x}_1 &= \Delta x_2 \\ \Delta\dot{x}_2 &= \frac{k_\delta}{m}\Delta x_1 - \frac{k_i}{m}\Delta x_3 \\ \Delta\dot{x}_3 &= \frac{k_i}{L}\Delta x_2 - \frac{R}{L}\Delta x_3 + \frac{1}{L}\Delta u \end{aligned}\right. \tag{11}$$

where $k_i = \left(2k_a i_0\right)/\delta_0^2$ and $k_\delta = \left(2k_a i_0^2\right)/\delta_0^3$.

Obviously system (11) is controllable. Thus its poles can be arbitrarily placed with the following control law [21]

$$\Delta u = r - k_1\Delta x_1 - k_2\Delta x_2 - k_3\Delta x_3 \tag{12}$$

Table

Parameters of the LSM and the sleeper

Parameter	Value	Parameter	Value
λ	400(mm)	l	500(mm)
d	50(mm)	w	100(mm)
n	8	B_r	1.085(T)
R	3(Ω)	m	1000(kg)
k_a	0.0025	g	10(m/s^2)

Choose the parameters as shown in Table for the system. Under the performance requirements proposed in [19], the closed-loop poles can be chosen as

$$p = \begin{bmatrix} -40 & -45 & -200 \end{bmatrix}^T \tag{13}$$

Then the following control parameters can be obtained

$$k_1 = -436208, \quad k_2 = -8817, \quad k_3 = 122 \tag{14}$$

4.3. Performance testification under $F_z = 0$

Utilizing controller Eq. (12) with parameters Eq. (14) in system (9) with $F_z = 0$ yields the response of the suspension gap shown in Fig. 5.

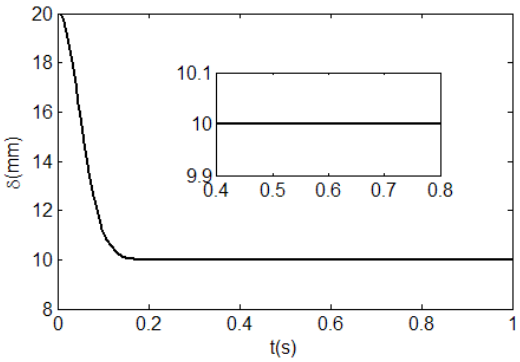

Fig. 5 Response of the suspension gap when $F_z = 0$

It can be seen from Fig. 5 that the performance is good and the response of the suspension gap is satisfactory even in enlarged view under the condition that the attraction force F_z generated by the sleepers is ignored.

4.4. Performance testification under $F_z \neq 0$

In experiment setup, z in Eq. (8) and x_1 in Eq. (9) satisfy the following equation

$$z + x_1 = a, \quad a = 0.12 \tag{15}$$

Moreover the variable y in Eq. (8) denotes the position of the vehicle on the guideway. For simplicity, let the speed of the vehicle is 1 m/s , then

$$y = t \tag{16}$$

Substituting parameters in Table, Eqs. (15) and (16) to (8) yields

$$F_z = 48.3\left(\frac{\pi}{2} - sin(10\pi t)\right)e^{10\pi x_1} \tag{17}$$

Utilizing controller Eq. (12) with parameters Eq. (13) in system Eq. (9) with F_z described in Eq. (17) yields the response of the suspension gap shown in Fig. 6.

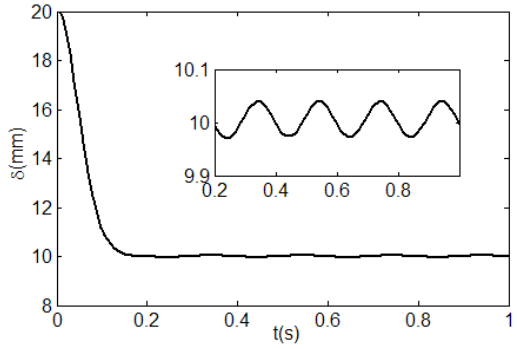

Fig. 6 Gap Response by typical state feedback when $F_z \neq 0$

It can be seen from Fig. 6 that the system can also be stabilized around $\delta_0 = 10$ mm using full state feedback controller when F_z is considered. But the performance is not satisfactory. In the enlarged view, resonance can be seen. And the amplitude of the resonance is about 0.05 mm. Although the resonance is small and passengers cannot feel it, it is bad for the suspension system. The resonance can be amplified under some unexpected situation, such as the elasticity of the guideway, disturbance from the wind and so on. Also, the frequency of the resonance is proportion to the speed of the vehicle, which increases the possibility of unsatisfactory performance.

5. Control design to reject the effect of the sleepers on the guideway

Substituting Eq. (8) into Eq. (9), the model of a single-point suspension system can be rewritten as

$$\left\{\begin{array}{l} \dot{x}_1 = x_2 \\ \dot{x}_2 = g - \dfrac{k_a}{m}\left(\dfrac{x_3}{x_1}\right)^2 - k_s e^{2kx_1} \\ \dot{x}_3 = \dfrac{x_2 x_3}{x_1} - \dfrac{x_1}{2k_a}(u - Rx_3) \\ y = x_1 \end{array}\right\} \tag{18}$$

where

$$k_s = \frac{B_0^2 l\, sin(kw)e^{-2ka}}{4mk\mu_0} cos(2ky + kw) + \frac{B_0^2 lwe^{-2ka}}{4m\mu_0} \tag{19}$$

In the expression k_s, y is the only variable. In experimental setup, there is position and speed detection system, from which y can be directly measured. Then k_s can be regarded as a known parameter.

It is surmised that the resonance shown in Fig. 6 results from the strong nonlinearity shown in Eq. (18). To reject the resonance, a nonlinear controller will be designed by feedback linearization. One reason to use feedback linearization is that it provides a technique for designing and synthesizing nonlinear systems by linear control theory, and the other reason is that it is simple to implement, which is quite important for the current experimental setup.

The first step is to check if the system (18) is feedback linearizable or not. Considering the following nonlinear SISO system

$$\begin{cases} \dot{x} = f(x) + g(x)u \\ y = h(x) \end{cases} \tag{20}$$

where $x \in R^n$, $f(x)$ and $g(x)$ are sufficiently smooth on a domain $D \subset R^n$, and $u \in R^1$ is a control function. The nonlinear system could be feedback linearized by input-state if and only if there exists a region $\Omega \in R^n$, in which the following two conditions hold [22-25].

The vector fields $\{g, ad_f g, ..., ad_f^{n-1} g\}$ linearly independent in Ω.

The set $\{g, ad_f g, ..., ad_f^{n-2} g\}$ involved in Ω.

It is easy to check that system (18) satisfies the above conditions i and ii. And the transformation matrix T can be obtained as

$$z = T(x) = \begin{bmatrix} x_1 \\ x_2 \\ g - \dfrac{k_a}{m}\left(\dfrac{x_3}{x_1}\right)^2 - k_s e^{2kx_1} \end{bmatrix} \tag{21}$$

Substituting Eq. (21) into system (18) yields the following linear model

$$\left.\begin{aligned} \dot{Z} &= \begin{bmatrix} 0 & 1 & 0 \\ 0 & 0 & 1 \\ 0 & 0 & 0 \end{bmatrix} Z + \begin{bmatrix} 0 \\ 0 \\ 1 \end{bmatrix} v \\ y &= \begin{bmatrix} 1 & 0 & 0 \end{bmatrix} Z \end{aligned}\right\} \tag{22}$$

where $u = \alpha(x) + \beta(x)v$, and

$$\left.\begin{aligned} \alpha(x) &= Rx_3 + 2mkk_s \frac{x_1 x_2}{x_3} e^{2kx_1} \\ \beta(x) &= \frac{mx_1}{x_3} \end{aligned}\right\} \tag{23}$$

It is obvious that linear system (22) is controllable. Then the following controller can be obtained choosing the same closed-loop poles described in Eq. (13)

$$v = r - 359999 z_1 - 18799 z_2 - 285 z_3 \tag{24}$$

Combining Eq. (23) and Eq. (24) yields the resultant controller

$$u = \alpha(x) + \beta(x)(r - 359999 z_1 - 18799 z_2 - 285 z_3) \tag{25}$$

where Z is determined by Eq. (21).

Utilizing controller Eq. (25) in system Eq. (18), the response of the suspension gap under the nonlinear controller for the suspension system (18) with consideration of the sleepers on the guideway can be obtained as shown in Fig. 7.

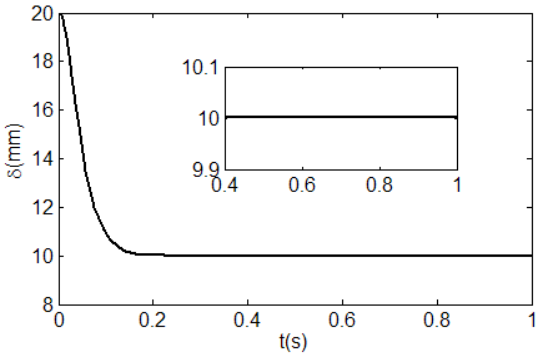

Fig. 7 Gap Response by feedback linearization when $F_z \neq 0$

It can be seen from Fig. 7 that the suspension performance is satisfactory using the proposed feedback linearization controller with consideration of the effect of the sleepers on the guideway. Comparing Fig. 5 with Fig. 7, it can be concluded that the proposed control algorithm is better than typical state feedback control strategy. And the obtained nonlinear controller can entirely reject the resonance caused by the effect of the sleepers.

6. Conclusion

In this work, an engineering problem is proposed and solved for LSM with PM Halbach located on the vehicle and ironless coils on the guideway. This kind of LSM has been utilized in GA maglev vehicle. It is a good candidate for propulsion system. Above all, the effect of the sleepers on the guideway is investigated. And the following results are obtained. First, the closed-form of the attractive force is deduced from the expression of the magnetic field of Halbach array. Second, the analytical result is added to a suspension system, the result of which shows the phenomenon of resonance. That is to say the typical state feedback control strategy can not guarantee the suspension performance while there are iron sleepers on the guideway. The proposed analytical model of the attractive force generated between the sleepers and the Halbach on the vehicle is simple, and suitable for analysis and controller design. Thus a nonlinear controller is designed using a feedback linearization technique. Simulation result shows the proposed control algorithm can effectively reject the resonance resulting from the effect of the sleepers on the guideway.

References

1. **Wu, X.M.** 2003. Maglev vehicles, Shanghai Science and Technology Press, Shanghai.

2. **Lee, H.W.; Kim, K.C.; Lee, J.,** 2006. Review of maglev train technologies, IEEE Transactions on Magnetics 42(7): 1917-1925.

3. **Ohsaki, H.; Du, J.** 2004. Influence of eddy current induced in steel rails on electromagnetic force characteristics of ems maglev systems, in the 18th International Conference on Magnetically Levitated Systems and Linear Drives. Shanghai, China.

4. **Tang, R.** 2008. Modern Permanent Magnet Machines: Theory and Design, China Machine Press, Beijing.

5. **Wang, X.** 2007. Permanent Magnet Machines, China Electric Power Press, Beijing.

6. **Zhou, S.Z.; Dong, Q.F.** 2004. Super Permanent Magnets: Hard Magnetic Materials, Metallurgical Industry Press, Beijing.

7. **Halbach K.** 1985. Permanent magnets for production and use of high energy beams, in the Proceedings of the 8th International Workshop on Rare-earth Permanent Magnets.

8. **Bergh, H.; Kratz, R.; Jeter, P.L.** Magnetic Levitation and Propulsion System", United States Patent No. US6827022B2.

9. **Hoburg, J. F.** 2004. Modeling maglev passenger compartment static magnetic fields from linear Halbach PM arrays, IEEE Transactions on Magnetics 40(1): 59-64.

10. **Li, C.S., Wang, J.B.; Xia, P.C.; Yan, L.G.** 2008. Structure of linear PM Halbach array for EDS Maglev, in the 20th International Conference on Magnetically Levitated Systems and Linear Drives, Part: Vehicles and Levitation Guidance, 7-12.

11. **Xia; Z.P.; Zhu, Z.Q.; Howe D.** 2004. Analytical magnetic field analysis of Halbach magnetized permanent-magnet machines, IEEE Transactions on Magnetics 40(4): 1864-1872.

12. **Markovic, M.; Perriard, Y.** 2009. Optimization design of a segmented Halbach permanent-magnet motor using an analytical model, IEEE Transactions on Magnetics 45(7): 2955-2960.

13. **Xiao Zhang; Yungang Li; Hu Cheng; Hengkun Liu.** Analysis of the planar magnetic field of linear PM Halbach array, accepted by 2011 International Conference on Mechanical Materials and Manufacturing Engineering. Nanchang, China.

14. **Doll, D.W.; Kratz, R.; Newman, M.J.** 2004. Linear synchronous motor control for an urban maglev, in the 18th International Conference on Magnetically Levitated Systems and Linear Drives. Shanghai, China.

15. **Yasuda, Y.; Fujino, M.; Tanaka, M.** 2004. The first HSST Maglev commercial train in Japan, in the 18th International Conference on Magnetically Levitated Systems and Linear Drives. Shanghai, China.

16. **Federal Transit Administration Team.** 2002. Assessment of CHSST Maglev for U.S. Urban Transportation.

17. **Sanhui Zhang.** 1999. Electromagnetics. Tsinghua University Press. Beijing.

18. **Cizhang Feng.** 1980. Electromagnet Field. People's Education Press. Beijing.

19. **Liu, H.K.; Zhang, X.; Chang, W.S.** 2009. PID control to Maglev train system, in 2009 International Conference on Industrial and Information Systems.

20. **Zhang, X.; Tan, Y.; Li, Y. G.; Mareels, I.** 2010. On the modelling complexity and utility of an EMS system, The 49th IEEE Conference on Decision and Control.

21. **Richard, C.D.; Robert, H.B.** 2008. Modern Control Systems, Pearson Prentice Hall. Upper Saddle River.

22. **Khalil, H.K.** 2002. Nonlinear Systems, Prentice Hall. Upper Saddle River.

23. **Isidori.** 1999. Nonlinear Control Systems, Springer. London.

24. **Cheng, D.Z.; Hu, X.M.; Shen, T.L.** 2010. Analysis and design of nonlinear control systems, Science Press. Beijing.

25. **Chemachema, M.; Belarbi, K.** 2010. State feedback linearization-based neural network adaptive controller for a class of uncertain SISO non-linear systems, International Journal of Modelling, Identification and Control 11(1): 44-51.

Xiao Zhang, Hu Cheng, Yungang Li

GELEŽINIŲ PABĖGIŲ POVEIKIO PAŠALINIMO TRANSPORTO PRIEMONEI SU MAGNETINE PAGALVE VALDYMO ALGORITMAS NAUDOJANT LINIJINIUS SINCHRONINIUS VARIKLIUS SU NUOLATINIAIS HALBACHO MAGNETAIS IR GELEŽIES NETURINČIOMIS RITĖMIS

R e z i u m ė

Magnetiniam vagonų pakėlimui naudojant linijinius sinchroninius variklius su nuolatiniais Halbacho magnetais ir geležies neturinčias rites, traukos jėga gali būti sukurta tarp nuolatinio Halbacho magneto ant vagono ir geležinių pabėgių. Veikdama priešingai pakabos jėgoms, ši jėga didina pakabų apkrovas ir taip blogina pakabos charakteristikas. Šiame darbe yra tyrinėtas geležinių pabėgių įtaka magnetinio pakėlimo sistemai ir pasiūlytas kontrolinis algoritmas šiam efektui pašalinti. Pirmiausia, pritaikius nuolatiniam Helbacho magnetui magnetinio lauko lygtis, yra nustatyta traukos jėga tarp geležinių pabėgių ir

nuolatinių Halbacho magnetų. Suminei pakėlimo charakteristikai nustatyti traukos jėga pridėta prie pakėlimo valdymo sistemos. Panaudojus tipinę padėties grįžtamojo ryšio valdymo strategiją, pastebimas rezonansas, kai vagonas juda pro geležinius kelio pabėgius. Pabėgių poveikiui pakabos sistemai panaikinti, naudota grįžtamojo ryšio linearizacijos technika ir sukurtas netiesinis valdiklis. Skaitinio modeliavimo rezultatai rodo, kad pasiūlytas netiesinės kontrolės algoritmas gali efektyviai panaikinti pabėgių sukeltą bėgio rezonansą.

Xiao Zhang, Hu Cheng, Yungang Li

CONTROL ALGORITHM TO REJECT THE EFFECT OF IRON SLEEPERS FOR MAGLEV VEHICLE USING LSM WITH PM HALBACH AND IRONLES COIL

S u m m a r y

In the magnetic levitation (maglev) vehicle that utilizes LSM with permanent magnet (PM) Halbach and ironless coil, attractive force can be generated between the PM Halbach on the vehicle and the iron sleepers on the guideway. With a direction opposite to the suspension force, this attractive force correspondingly increases the suspension load and affects the suspension performance. In this work, the effect of iron sleepers on maglev suspension system is investigated, and a control algorithm is proposed to reject this effect. First, by introducing the magnetic field equation of the PM Halbach, the analytical expression of the attraction force between the iron sleepers and the PM Halbach array is obtained. Then the attraction force is added to the suspension control system, and the resultant suspension performance is presented. It is shown that resonance occurs when the vehicle passes through the iron sleepers on the guideway using typical state feedback control strategy. To reject the effect of the sleeps on the suspension system, a nonlinear controller using a feedback linearization technique is developed. Simulation result shows that the proposed nonlinear control algorithm can effectively reject the resonance resulted from the sleepers on the guideway.

Received March 21, 2011
Accepted December 15, 2011